Quantitative analysis of local fracture surface patterns in materials by shape parameters

M. TANAKA
Department of Mechanical Engineering, Faculty of Engineering and Resource Science, Research Institute of Materials and Resources, Akita University, 1-1 Tagatagakuen-cho, Akita 010-8502, Japan

Y. KIMURA
Nippon Systemware Company Ltd., 31-11 Sakuragaoka-cho, Shibuya-ku, Tokyo 150-8577, Japan

R. KATO
Department of Mechanical Engineering, Faculty of Engineering and Resource Science, Akita University, 1-1 Tagatagakuen-cho, Akita 010-8502, Japan

N. OYAMA
Department of Mechanical Engineering, Faculty of Engineering and Resource Science, Akita University, 1-1 Tagatagakuen-cho, Akita 010-8502, Japan

Geometrical features of fracture surfaces in materials can be described by shape parameters such as fractal dimension [1–12] and surface roughness [11–13]. The fractal dimension is an index which represents a self-similarity and a scale-independence in complex shapes of objects. The surface roughness describes the averaged magnitude of undulation on the surface, which depends on the dimension of analyzed objects. Thus, the fractal dimension and the surface roughness are very different shape parameters, and the local variations of these shape parameters may give important information about principal fracture mechanism or local fracture process in materials. In this study, computer programs were developed for calculating the fractal dimension and the surface roughness on small regions of fracture surfaces. These shape parameters were calculated using the height data of the three-dimensional fracture surfaces reconstructed by the stereo matching method [12]. The relative values of the shape parameters were displayed as two-dimensional images, namely, the fractal dimension map (FDM) and the surface roughness map (SRM) of 256 gray-scale levels. The local variations of these shape parameters were then examined on the three-dimensional fatigue fracture surface of a Cu-Be alloy. The FDM and the SRM were composed in order to detect characteristic fracture surface patterns such as brittle fracture surface and ductile fracture surface on the original image. Further, the area proportion of a specific fracture pattern was estimated according to the threshold values of the fractal dimension and the surface roughness.

Fig. 1 shows the procedure of the calculation and mapping of shape parameters in an image. The calculated region was moved in both x- and y-directions by k pixels in mapping process. The fractal dimension was estimated using the height data by the box-counting method [14]. The number of boxes, N, covering the fracture surface can be related to the box size, r, through the three-dimensional fractal dimension, D ($2 < D < 3$), by the following power law relationship:

$$N \propto r^{-D} \tag{1}$$

The fractal dimension, D_b, can be calculated from Equation 1 by the regression analysis using the datum sets of N and r. The surface roughness, rms, in a given area of $m \times m$ in pixel was calculated by the following Equation 11:

$$\mathrm{rms} = \sqrt{\sum_{x=1}^{m}\sum_{y=1}^{m}\frac{\{z(x,y) - Z'\}^2}{m^2 - 1}} \tag{2}$$

where $z(x, y)$ is the height of a point $P(x, y)$ and $Z' = \sum_{i=1}^{m}\sum_{j=1}^{m}\frac{z(i,j)}{m^2}$.

Fig. 2 shows the result of geometrical analysis on the stage I fatigue fracture surface of a Cu–Be alloy [12]. The original image is the computed area for three-dimensional image reconstruction (Fig. 2a). The crack growth direction is approximately from right to left in the figure. The height image is displayed as an image of 256 gray-scale level, and the higher part is shown by the brighter region in the image (Fig. 2b). The brighter region in FDM (Fig. 2c and e) or SRM (Fig. 2d and f) shows the region of the larger value of the shape parameter. The actual values of shape parameters and the imaging condition of FDM and SRM are also shown in the figure. The stage I fatigue fracture surface is for the most part formed by ductile fracture with slip steps and dimples except a small amount of grain-boundary facets (for example, enclosed by broken lines in Fig. 2) [12]. Therefore, the bright regions of the ductile fracture prevail in FDM, while the parts of the ductile fracture do not always exhibit a bright contrast in SRM. The regions enclosed by broken lines in both maps indicate the flat parts, which correspond to grain-boundary facets. These principal features of the fracture surface

0022–2461

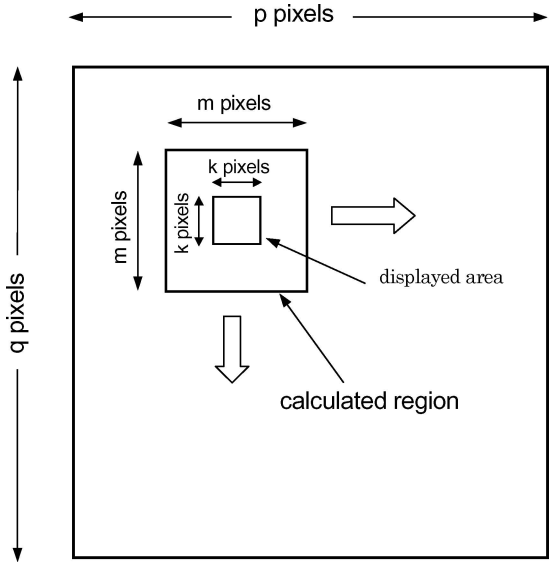

Figure 1 Schematic illustration of the displayed area ($k \times k$ in pixel) centered at the calculated region ($m \times m$ in pixel) in an image ($p \times q$ in pixel) in the calculation and mapping of shape parameters.

are almost unchanged with the imaging condition (m and k in Fig. 1) of FDM (Fig. 2c and e) and SRM (Fig. 2d and f). The grain-boundary facets are also shown in the original image (Fig. 2a). The flat region seems to exhibit a dark contrast in both FDM and SRM. Other features are steps (steeply inclined parts) that are dark in FDM and very bright in SRM. Characteristic fracture surface patterns in some materials including the Cu–Be alloy are shown in FDM and SRM as follows (Table I).

TABLE I Summary of characteristic fracture surface patterns shown in the fractal dimension map (FDM) and the surface roughness map (SRM)

Fracture surface patterns	FDM	SRM
Region of relatively complex geometry such as a ductile fracture surface	Bright	Not always bright
Relatively flat region such as a brittle fracture surface	Dark	Dark
Steeply inclined part like a step	Dark	Bright

(1) An area which shows bright contrast in FDM but not always in SRM, corresponds to a region of relatively complex geometry such as a ductile fracture surface.
(2) A region which shows dark contrast in both FDM and SRM, corresponds to a relatively flat region such as a brittle fracture surface.
(3) An area which shows dark contrast in FDM and bright contrast in SRM, corresponds to a steeply inclined part like a step. This part apparently shows the

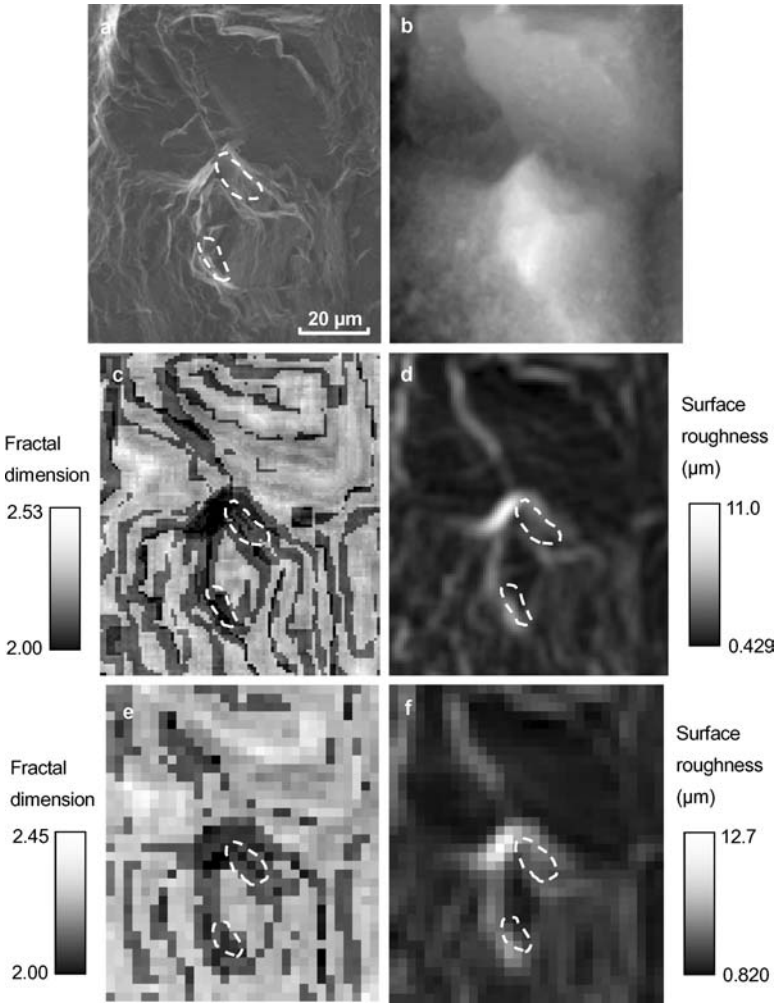

Figure 2 Result of geometrical analysis on the stage I fatigue fracture surface of a Cu–Be alloy (fatigued by repeated bending at the maximum total strain range ($\Delta\varepsilon_t$) of 0.0171) [12]. (a) Original image; (b) height image; (c and e) FDM; and (d and f) SRM (the imaging condition (Fig. 1) is $m = 24$ and $k = 4$ in pixel for (c) and (d), and $m = 36$ and $k = 12$ in pixel for (e) and (f) (some grain-boundary facets are enclosed by broken lines).

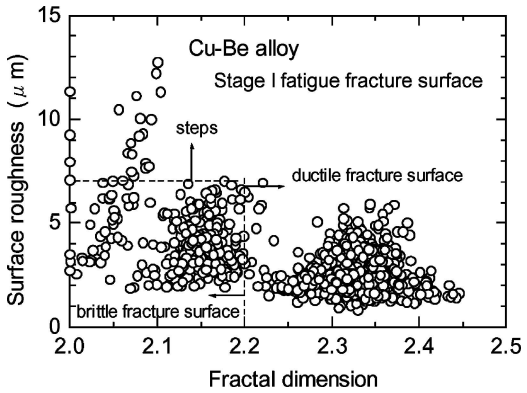

Figure 3 The relationship between the fractal dimension and the surface roughness in small regions of the stage I fatigue fracture surface (Fig. 2) in a Cu–Be alloy (the analyzed fracture surface is 372 × 432 in pixel, and the condition of the calculation is $m = 36$ and $k = 12$ in pixel).

smaller fractal dimension and the larger surface roughness, irrespective of fracture mechanisms.

It should be noted that these three features in FDM and SRM are non-overlapping in any case. Therefore, fracture patterns in small regions can be visually known from inspection of these features in FDM and SRM.

The area proportion of a specific fracture surface patterns can be known by calculating the shape parameters in the small regions (Fig. 3). The analyzed area of the fracture surface (372 × 432 in pixel and almost the same as Fig. 2b) was divided into 1116 small regions. Relatively large values of the size of the calculated area ($m = 36$ pixels) and that of the small regions ($k = 12$ pixels) were chosen in the calculation in order to extract principal features of local fracture surface patterns in FDM and SRM (Fig. 2e and f). In the Cu–Be alloy the fractal dimension of the fracture surface profile (D', $1 < D' < 2$) was in the range from 1.190 to 1.210 for the stage I fatigue fracture surface in which the ductile fracture mechanism prevailed [12], whereas the value of D' was 1.168 for the stage II fatigue fracture surface formed by grain-boundary fracture (brittle fracture) [8]. It is assumed in this study that an area in which the fractal dimension of the three-dimensional fracture surface (D, $2 < D < 3$) is less than 2.20, belongs to the brittle fracture surface, while an area in which the value of the surface roughness (rms) is more than about 7.0 μm, is regarded as a step. The area proportion is 70.1% for the ductile fracture surface, 27.9% for the brittle fracture surface and 2.0% for steps. If the steps are excluded in the estimation, the area proportion of the brittle fracture surface is 28.5% (that of the ductile fracture surface is 71.5%).

If all steps on the fracture surface are formed in a ductile manner, for example, by anti-plane shear mode (mode III) [15], the steps should be classified into the ductile fracture surface. The area proportion of the grain-boundary fracture surface gives the minimum value (27.9%) in this case. Steeply inclined parts on the fracture surface may also be formed by grain-boundary fracture. If these parts belong to the grain-boundary facets, the area proportion of the brittle fracture surface gives the maximum value (29.9%). Some of the steeply inclined parts may belong to the ductile fracture surface, while others should be classified into the brittle fracture surface. The true area proportion of the brittle fracture surface may lie between the minimum value (27.9%) and the maximum value (29.9%) in this case. In general, the moderate calculation condition and the exact threshold values of the fractal dimension and the surface roughness should be chosen for classification of different fracture patterns (for example, ductile fracture surface, brittle fracture surface or step). Thus, the geometrical analysis by shape parameters can be applied not only to the detection of characteristic fracture patterns but also to the quantitative evaluation of the specific fracture surface patterns in materials.

Acknowledgment

The authors thank the Iron and Steel Institute of Japan for financial support.

References

1. B. B. MANDELBROT, D. E. PASSOJA and A. J. PAULLAY, *Nature* **308** (1984) 721.
2. E. E. UNDERWOOD and K. BANERJI, *Mater. Sci. Eng.* **80** (1986) 1.
3. R. H. DAUSKARDT, F. HAUBENSAK and R. O. RITCHIE, *Acta Metall.* **38** (1990) 142.
4. S. MATSUOKA, H. SUMIYOSHI and K. ISHIKAWA, *Trans. Jpn. Soc. Mech. Eng.* **56** (1990) 2091.
5. M. TANAKA, *J. Mater. Sci.* **27** (1992) 4717.
6. V. Y. MILMAN, N. A. STELMASHENKO and R. BLUMENFELD, *Progress Mater. Sci.* **38** (1994) 425.
7. P. STREITENBERGER, D. FÖRSTER, G. KOLBE and P. VEIT, *Scripta Metall. Mater.* **33** (1995) 541.
8. M. TANAKA, A. KAYAMA and R. KATO, *J. Mater. Sci. Lett.* **18** (1999) 107.
9. X. W. LI, J. F. TIAN, S. X. LI and Z. G. WANG, *Mater. Trans.* **42** (2001) 128.
10. U. WENDT, K. STIEBE-LANGE and M. SMID, *J. Microscopy* **207** (2002) 169.
11. N. ALMQVIST, *Surface Sci.* **355** (1996) 221.
12. M. TANAKA, Y. KIMURA, L. CHOUANINE, J. TAGUCHI and R. KATO, *ISIJ Int.* **43** (2003) 1453.
13. A. W. ORLOWICZ and M. MROZ, *Z. Metallkd.* **94** (2003) 1320.
14. M. TANAKA, Y. KIMURA, L. CHOUANINE, R. KATO and J. TAGUCHI, *J. Mater. Sci. Lett.* **22** (2003) 1279.
15. D. Hull, in "Fractography" (Cambridge University Press, Cambridge, 1999) p. 91.

Received 12 August
and accepted 17 November 2004